

Removal of Canvas Patterns in Digital Acquisitions of Paintings

Bruno Cornelis, *Member, IEEE*, Haizhao Yang*, Alex Goodfriend, Noelle Ocon, Jianfeng Lu,
and Ingrid Daubechies, *Fellow, IEEE*

Abstract—We address the removal of canvas artifacts from high-resolution digital photographs and X-ray images of paintings on canvas. Both imaging modalities are common investigative tools in art history and art conservation. Canvas artifacts manifest themselves very differently according to the acquisition modality; they can hamper the visual reading of the painting by art experts, for instance, in preparing a restoration campaign. Digital removal of canvas is desirable for restorers when the painting on canvas they are preparing to restore has acquired over the years a much more salient texture. We propose a new algorithm that combines a cartoon-texture decomposition method with adaptive multiscale thresholding in the frequency domain to isolate and suppress the canvas components. To illustrate the strength of the proposed method, we provide various examples, for acquisitions in both imaging modalities, for paintings with different types of canvas and from different periods. The proposed algorithm outperforms well-known methods such as Morphological Component Analysis (MCA) and Wiener filtering.

Keywords—*Digital painting analysis, canvas removal, denoising, periodic noise, source separation*

I. INTRODUCTION

Computer processing of digitized artworks is a fast growing and challenging field of research. A number of algorithms were proposed to analyze high-resolution

digital images of paintings in support of art scholarship. Examples include the numerical characterization of painting style [1], [2], [3] for the authentication or dating of paintings, canvas thread counting [4], [5], [6], [7] for art forensics, and the (semi-) automatic detection and digital inpainting of cracks [8], [9], [10]. In the domain of image enhancement, the algorithmic removal of cradling artifacts within X-ray images of paintings on panel was studied, mostly to facilitate the reading of the painting by art experts [11], [12], but also to improve the performance of the crack detection method presented in [9].

This paper concerns the removal of canvas artifacts from both high-resolution digital photographs and X-ray images of paintings on canvas. Canvas removal can help in the reading of the painting by art experts for instance during a restoration campaign, to assist in the interpretation of the artists' creative intent, or in art historical studies. Initially, the question of removing canvas from high-resolution photographs was raised for the painting *Portrait of Suzanne Bambridge* (1891) made by Paul Gauguin (1848-1903) in Tahiti [13], which is in dire need of restoration and where the prominent grid-like structure caused by the underlying jute canvas is quite disturbing (see Fig. 1). In lining the painting, the original canvas was pressed into the pictorial layer, accentuating the grid-like canvas structure. This restoration procedure consists of applying a heated wax or resin to the back of the original canvas in order

Manuscript received XXX; revised XXX. * Corresponding author: Haizhao Yang



Fig. 1. *Portrait of Suzanne Bambridge*: (left) high resolution photography, (right) detail under raking light clearly showing canvas texture and brushstrokes [14].

to stabilize any loose paint and to prevent any future losses. The removal of the prominent and very regular canvas pattern helped in the analysis of the painting's structural condition and the uncovering of restoration areas.

When an artist chooses to paint his subject on canvas, (s)he is aware of the texture this will convey to the finished painting and typically factors this in when realizing the artwork. However, over time this natural texture may be altered by various external factors. Dirt accumulated in the valleys between the threads of the canvas can get trapped by later applications of varnish after imperfect cleaning. In addition, layers of varnish, always slightly thicker in the inter-thread spacings than on top of the threads become visually more prominent by the unavoidable yellowing of the aging varnish, thus emphasizing the thread structure.

X-ray radiographs provide conservators and art historians with information related to the three-dimensional structure of a painting, not just its surface. They are for example used to reveal changes between earlier paint layers and the final surface. The penetrating X-rays also provide information about structural aspects of paintings, such as the support layer (i.e. the threads in paintings on canvas or the wood grain, joints or splits

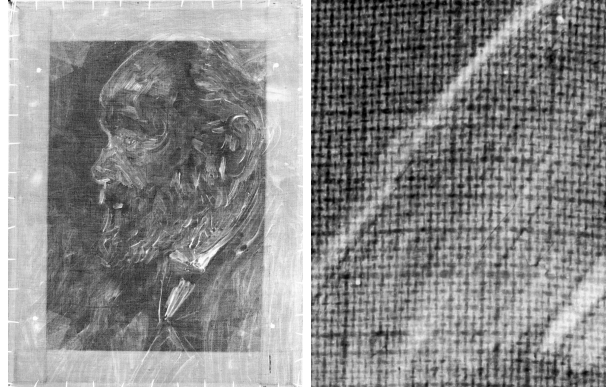


Fig. 2. X-ray image of van Gogh's painting *Portrait of an Old Man with Beard*, 1885, Van Gogh Museum, Amsterdam (F205).

in paintings on wood panel), but also about cracks and losses in the ground and paint layers. The greater the radiographic absorption of the material, the greater the opacity, meaning that the X-ray image intensity varies according to not only paint thickness variations but also to composition of the material. This investigative imaging technique is therefore an important aid for modern-day conservators and art historians. Fig. 2 shows an X-ray image of a canvas painting by *van Gogh* where the canvas and stretcher of the painting are very prominent.

Digitally removing canvas artifacts is not straightforward since the canvas weave often only deviates from truly horizontal and vertical directions, but also may fail to be straight-lined (see Fig. 2); in addition, the spacing between threads is typically not exactly periodic. These deviations from perfect regularity in the canvas are exploited in [15], [5]. Next to these local deviations in periodicity, the canvas can suffer from even stronger deformations at the edges of the stretcher where it was attached, a phenomenon also known as cusping. An additional challenge lies in the fact that these canvas artifacts manifest differently according to the pictorial context and modality. In X-ray images especially, the presence of canvas can dominate in areas where the paint is X-ray transparent, while areas of more opacity

would show less interference of the canvas pattern.

We propose a method for the canvas removal problem that can be deployed for both high-resolution photographs and X-ray images of canvas paintings. In a first stage we decompose the image into a cartoon and a texture component. The cartoon component retains strong edges, mostly from the painting composition, while the texture component consists of the canvas as well as a plethora of other features such as fine-scale brushstrokes, cracks, etc. In a second stage we focus on the texture component, from which we isolate the canvas by localizing and suppressing the frequency components from the canvas. The residual is fed back to the cartoon components giving us the final painting image, free of canvas. The results of our method were evaluated in two ways. On one hand, we printed on canvas a high-resolution scan of a painting on masonite, and applied our algorithm to a scan of the print, which we then compared to the original. In this case, the original scan can be viewed as a “ground truth”; however, the printing process itself introduces additional variation that produces extra, non-canvas “noise”, confounding SNR measurements. On the other hand, we also worked with art experts to evaluate our algorithm. They compare our proposed method with other competing methods (see Section II) and we explored criteria to quantify the advantages and shortcomings of each approach, with the aim of devising a method that would use each approach in portions of the painting where it is most successful.

The paper is organized as follows. In Section 2 we will introduce related work and state-of-the-art algorithms. In Section 3 we will introduce the proposed algorithm together with a detailed explanation of its parameters. In Section 4 we extensively test our algorithm and compare it with MCA and a smoothing Wiener filter approach, first presented in [16]. Finally, the last section contains conclusions along with some ideas for future work regarding this novel application.

II. RELATED WORK AND STATE-OF-THE-ART

Several solutions for the removal of periodic (or quasi-periodic) noise have been proposed in the literature, such as frequency domain median filters [17], [18], notch filters, a Gaussian notch reject filter (GNF) and its improvement, the Windowed GNF [19]. However, none of them are readily applicable due to the highly specific nature of canvas contamination. This led the authors of [16] (including one of us) to propose a new generic way of periodic noise filtering for removing canvas contamination in high-resolution photographs of paintings. Canvas removal was approached in [16] as a denoising problem, i.e, the *uncompromised* painting image \mathcal{I}^p is retrieved from the *contaminated* image $\mathcal{I} = \mathcal{I}^p + \mathcal{I}^c$, where the underlying support is represented by an additive (periodic) noise component \mathcal{I}^c (canvas), which is locally independent of the painting signal \mathcal{I}^p . Therefore, a *smoothing Wiener filter* was proposed, defined in the frequency domain as:

$$H_W(\xi) = \frac{S_{\mathcal{I}^p}(\xi)}{S_{\mathcal{I}^p}(\xi) + S_{\mathcal{I}^c}(\xi)},$$

with $\xi \in \mathbb{R}^2$ the variable in the two-dimensional frequency domain, $S_{\mathcal{I}^p}(\xi)$ the power spectral density (PSD) of the uncontaminated image, and $S_{\mathcal{I}^c}(\xi)$ the PSD of the canvas. Subsequently, a quad-tree decomposition of the entire image was constructed and the filter strength adapted according to the degree of canvas contamination determined per quad-tree block. The overall Wiener filter was designed to specifically target the removal of independent periodic noise caused by the canvas without affecting the finer structures of the painting (e.g. brushstrokes, cracks, previous restorations or details). Even though robust to slight deviations in thread density and orientation, this approach fails in cases where the canvas is heavily distorted, due to cusping for example, and with other than plain-weave canvases. Moreover, the method was designed for high-resolution photographic material and not for

X-ray images where the canvas dominates and is much more sharply delineated.

In [20], [21] a source separation algorithm called *morphological component analysis* (MCA) is introduced. MCA successfully decomposes an image $\mathcal{I} = \mathcal{I}^{cart} + \mathcal{I}^{txt}$ into its constituents, assuming that \mathcal{I}^{cart} and \mathcal{I}^{txt} have sparse decompositions in different standard dictionaries, called D_{cart} and D_{txt} respectively. In our case, the canvas texture could be sparsely represented in a dictionary of high frequency curvelets, shearlets, wavelet packets or a discrete cosine transform (DCT) while the painting can be sparsely represented using a dual-tree complex wavelet transform (DT-CWT) [22], which is optimal for the representation of piecewise smooth signals. To illustrate the strength of MCA an example is given in [20] where canvas is artificially introduced into a photograph and subsequently removed by using the curvelet and DCT dictionaries. However, the canvas used in that example is very regular and this toy example is far from representative for a real-life scenario. After extensive experimental evaluation we found that for images of real-life paintings, the best performing two dictionaries are the discrete cosine transform and the dual-tree complex wavelet transform; the latter is the same dictionary as in [11] for the painting content. The canvas image \mathcal{I}^{txt} can be sparsely represented in the first dictionary, and the paint image \mathcal{I}^{cart} in the second; neither component has a sparse expansion in the other dictionary. Even though MCA is a very powerful all-round method, its performance depends strongly on the choice of dictionaries used to represent each component. Its lack of parametrisation makes it an unwieldy technique as it often tends to remove other fine-scale features within the painting (see Section IV for more details). Moreover, MCA fails in removing the canvas completely within X-ray images when the canvas weave is strongly non-periodic.

III. PROPOSED ALGORITHM

We formulate the digital canvas removal problem as a source separation problem for extracting sources with periodic structures. We will restrict our discussion to the analysis of grayscale images and omit explicit modeling of color images, since the method for grayscale images can be applied to each individual channel of the color image. Let \mathcal{I} denote the intensity of a grayscale image of a painting, e.g. an X-ray image (see Fig. 2 for an example). The image data \mathcal{I} usually contains several components. In case of a photograph we observe the surface layer, the paint, canvas, possible damage such as cracks, and restorations. For X-ray images of canvas paintings, additional components, such as the primer between the canvas threads and wooden stretchers, become visible due to greater transparency of the surface layers to X-rays. Some types of damage, such as cracks and areas of missing paint, are usually highly contrasted within the X-ray modality. Additionally, various types of noise can be introduced during the acquisition process. Hence, we model the image data \mathcal{I} as an additive superposition of three parts:

$$\mathcal{I} = \mathcal{I}^p + \mathcal{I}^c + \mathcal{I}^{out},$$

where \mathcal{I}^p denotes the paint layer; \mathcal{I}^c represents the canvas texture; and the summation of the other outlier components is denoted as \mathcal{I}^{out} . The quantitative canvas analysis in [6] models the canvas part as $\mathcal{I}^c(x) := a(x)S(2\pi N\phi(x))$, where S is a periodic shape function on the square $[0, 2\pi]^2$ reflecting the basic weave pattern of the canvas (see [23] for its definition); $a(x)$ is a slowly varying function accounting for the variations of the amplitude of the canvas due to the influence of the paint layer and the reflection of light in the acquisition process; $\phi(x)$ is a smooth deformation describing the local warping of the canvas; and N is a density parameter describing the averaged overall weave density of the canvas. We can further simplify this model by applying the algorithms presented in [8], [9], [10], [11], [12],

designed to precisely remove components in \mathcal{I}^{out} such as the wooden stretcher and cracks.

A straightforward idea for canvas removal is to estimate the phase function $N\phi(x)$, the shape function $S(x)$ and the amplitude function $a(x)$ directly from a given image \mathcal{I} . It has been shown in [6] that the two-dimensional synchrosqueezed transforms [24], [25] are powerful tools in estimating the phase function $N\phi(x)$. However, although there exist algorithms for estimating $S(x)$ and $a(x)$ in one-dimensional problems [26], [27], there is no efficient method suitable for the two-dimensional problem encountered here, where the image contains structured noise, such as brushstrokes, cracks, and stretchers in \mathcal{I}^p and \mathcal{I}^{out} .

By rewriting the canvas part in terms of the Fourier series of the shape function $S(x)$, i.e.,

$$\mathcal{I}^c(x) = \sum_{n \in \mathbb{Z}^2} a(x)\widehat{S}(n)e^{2\pi i N n \cdot \phi(x)},$$

we see that canvas removal is equivalent to removing the deformed plane waves $a(x)\widehat{S}(n)e^{2\pi i N n \cdot \phi(x)}$, corresponding to peaks in the Fourier domain (see Fig. 3 (d) for an example). In places where the canvas is deformed, due to irregularities in the canvas weave, attaching the canvas to its stretcher or previous conservation practice, peaks can be spread out and we can even observe ridges in the frequency domain. Therefore, we conclude that canvas removal is equivalent to peak and ridge removal in the frequency domain.

Based on the above observations, we propose a two-stage method for canvas removal as follows.

A. Cartoon-Texture Decomposition

In the first stage of our algorithm, we apply well-established cartoon-texture decomposition methods to estimate the cartoon part \mathcal{I}^{cart} of \mathcal{I} , i.e. we decompose \mathcal{I} as

$$\mathcal{I} = \mathcal{I}^{cart} + \mathcal{I}^{txt}.$$

Due to the oscillatory nature of canvas patterns, the canvas component \mathcal{I}^c together with some other fine

features (e.g., cracks, brushstrokes) will be contained in \mathcal{I}^{txt} . In contrast to simple low-pass filters, cartoon-texture decomposition methods permit sharp edges of complex geometry in the cartoon part. This is especially important for high-resolution digital photographs, where the painting image contains sharp contours and crisp edges. This asset reduces the influence of horizontal and vertical edges in the painting part \mathcal{I}^p during the estimation of the canvas texture.

A general variational framework of the cartoon-texture decomposition aims at solving the following optimization problem:

$$\inf_{(u,v) \in X_1 \times X_2} \{\lambda F_1(u) + F_2(v) : f = u + v\}, \quad (1)$$

where f is the given image, λ is a tuning parameter, F_1 , $F_2 \geq 0$ are functionals and X_1 , X_2 are function spaces such that any function pair $(u, v) \in X_1 \times X_2$ satisfies $F_1(u) < +\infty$ and $F_2(v) < +\infty$. By choosing a proper functional F_1 that favors piecewise smooth functions u and another F_2 that favors oscillatory functions v , i.e., $F_1(u) \ll F_1(v)$ and $F_2(v) \ll F_2(u)$, one can decompose the given image f into its cartoon part u and texture part v by solving the above optimization problem [28].

There has been extensive research in designing functionals F_1 and F_2 in terms of decomposition accuracy and computational efficiency depending on different applications [29], [30], [31], [28], [32]. In what follows, we will apply the efficient nonlinear filtering cartoon-texture decomposition method of [32], which can be rapidly solved in the Fourier domain. The authors in [32] proposed a simple model with $X_1 \times X_2 = H^1 \times H^{-1}$ and $F_1 \times F_2 = \|\cdot\|_{H^1} \times \|\cdot\|_{H^{-1}}$. The solution u to the optimization in (1) is $\widehat{u} = \widehat{L}_\lambda \widehat{f}$, where

$$\widehat{L}_\lambda(\xi) = \frac{1}{1 + \lambda(2\pi|\xi|)^4}.$$

Hence, the cartoon texture decomposition is $(u, v) = (\widehat{L}_\lambda * f, (\text{Id} - \widehat{L}_\lambda) * f)$, which are two complementary components obtained by applying a low-pass and high-

pass filter. Here Id represents an identity map. However, this simple solution u does not preserve sharp edges. Based on the observation that the total variation of a cartoon region does not decrease by low-pass filtering and the total variation of a textured region decreases fast under low-pass filtering, the authors of [32] defined the local total variation (LTV) at a position x as

$$\text{LTV}_\lambda(f)(x) := L_\lambda * |Df|(x),$$

where Df is the derivative of f . Hence, the quantity

$$\gamma_\lambda(x) := \frac{\text{LTV}_\lambda(f)(x) - \text{LTV}_\lambda(L_\lambda * f)(x)}{\text{LTV}_\lambda(f)(x)}$$

quantifies the relative reduction of the local total variation by the low-pass filter L_λ . Therefore, the authors proposed a better solution to preserve strong edges in the cartoon part by a weighted average:

$$\begin{aligned} u(x) &= w(\gamma_\lambda(x))(L_\lambda * f)(x) \\ &\quad + (1 - w(\gamma_\lambda(x)))f(x), \\ v(x) &= f(x) - u(x), \end{aligned}$$

where $w(x) : [0, 1] \rightarrow [0, 1]$ is the increasing function defined by

$$w(x) = \begin{cases} 0 & x \leq 0.25 \\ 4x - 1 & 0.25 \leq x \leq 0.5 \\ 1 & x \geq 0.5 \end{cases}.$$

B. Peak and ridge removal

In the first stage, we decomposed the image data \mathcal{I} via a cartoon-texture decomposition as follows:

$$\begin{aligned} \mathcal{I}^{\text{cart}} &= w(\gamma_\lambda(x))(L_\lambda * \mathcal{I})(x) \\ &\quad + (1 - w(\gamma_\lambda(x)))\mathcal{I}(x), \\ \mathcal{I}^{\text{txt}}(x) &= \mathcal{I}(x) - \mathcal{I}^{\text{cart}}(x). \end{aligned}$$

The canvas part $\mathcal{I}^c = a(x)\widehat{S}(2\pi N\phi(x))$ is contained in \mathcal{I}^{txt} . In the second stage, we propose an adaptive multiscale thresholding algorithm for peak and ridge removal in the frequency domain, which is equivalent to removing canvas structure from \mathcal{I}^{txt} .

1) Peak and ridge estimation: Recall that we want to remove

$$\mathcal{I}^c(x) = \sum_{n \in \mathbb{Z}^2} a(x)\widehat{S}(n)e^{2\pi i N n \cdot \phi(x)},$$

from the texture part \mathcal{I}^{txt} after cartoon-texture decomposition. Due to other outlier components in \mathcal{I}^{out} , remaining traces of the cartoon part, and the deformation $N\phi(x)$, peaks and ridges are not prominent in the frequency domain (see Fig. 3(d), which shows the spectrum of the example in Fig. 12). To enhance the prominence of peaks and ridges we apply an anisotropic band-pass filter to $\widehat{\mathcal{I}}^{\text{txt}}$; more precisely we evaluate

$$\widehat{\mathcal{I}}^b = g_{\sigma_1} * \widehat{\mathcal{I}}^{\text{txt}} - g_{\sigma_2} * \widehat{\mathcal{I}}^{\text{txt}},$$

where g_{σ_1} and g_{σ_2} are two Gaussian filters with standard deviations σ_1 and σ_2 , and $\widehat{\mathcal{I}}^b$ is the filtered spectrum. Since canvas texture is usually a superposition of horizontal and vertical deformed plane waves, we project $\widehat{\mathcal{I}}^b$ along the horizontal and vertical axes and identify the peak positions of the projected one-dimensional signals. The peak positions along the horizontal axis are denoted as $\{\xi_{1i}\}$ while those for the vertical axis are denoted as $\{\xi_{2j}\}$. These peaks are illustrated in Fig. 3(a) and (b) for positive $\{\xi_{1i}\}$ and $\{\xi_{2j}\}$. Only empirically prominent peaks are considered situated at multiples of a fundamental frequency; other misleading peaks, generated by noise, are discarded. The peak positions $\{\xi_{1i}\}$ are multiples of the fundamental frequency $N\partial_{x_1}\phi(x)$ in the horizontal direction, while $\{\xi_{2j}\}$ are multiples of $N\partial_{x_2}\phi(x)$ in the vertical direction. Due to the deformation $\phi(x)$ of the canvas, we pick an area \mathcal{S}_r surrounding the peak and ridge position to cover the canvas component in the frequency domain as follows:

$$\begin{aligned} \mathcal{S}_r &:= \{\xi = (\xi_1, \xi_2) : |\xi_1 - \xi_{1i}| \leq r \text{ for some } i \\ &\quad \text{or } |\xi_2 - \xi_{2j}| \leq r \text{ for some } j\}, \end{aligned}$$

where r is a parameter measuring the texture deviation caused by the deformation $\phi(x)$; the larger the deviation, the larger r is chosen. In most numerical

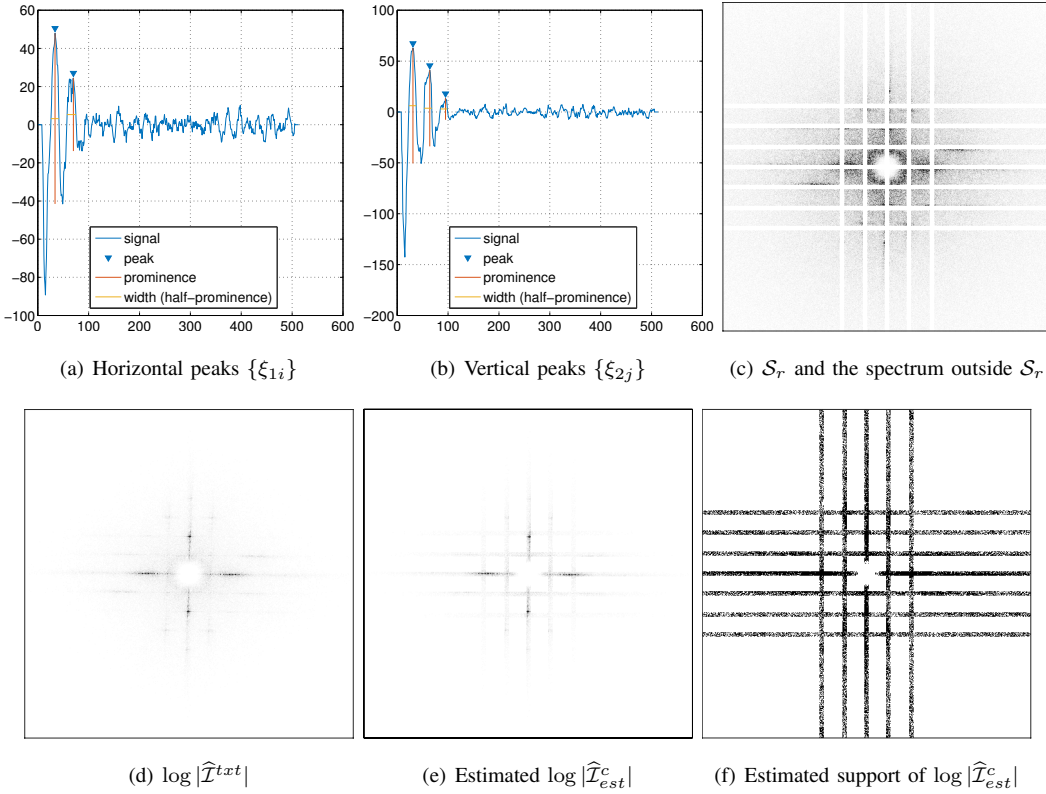


Fig. 3. Peak and ridge detection in the frequency domain. (a) and (b) show the projected spectrum of $|\widehat{\mathcal{I}}^{txt}|$ in (d) along the horizontal axis and the vertical axis, respectively. (e) shows the estimated spectrum $\widehat{\mathcal{I}}_{est}^c$ by thresholding $\widehat{\mathcal{I}}^{txt}$. (c) shows the S_r estimated from $\widehat{\mathcal{I}}^{txt}$ and the spectrum outside S_r . (f) shows the estimated support of the spectrum $|\widehat{\mathcal{I}}_{est}^c|$.

experiments, r is set to be 2, 3, or 4. As shown in Fig. 3(c) and (d), the estimated S_r essentially covers the support of $\widehat{\mathcal{I}}^c$ in the frequency domain.

2) *Multiscale adaptive thresholding:* A simple idea following the peak and ridge estimation is to threshold the restriction of $\widehat{\mathcal{I}}^{txt}$ to S_r . Suppose $\widehat{\mathcal{I}}_{est}^c(\xi)$ is the estimated spectrum of \mathcal{I}^c . This simple idea is equivalent to defining $\widehat{\mathcal{I}}_{est}^c(\xi) = \widehat{\mathcal{I}}^{txt}(\xi)$ if $|\widehat{\mathcal{I}}^{txt}(\xi)| > \delta$ and letting $\widehat{\mathcal{I}}_{est}^c(\xi) = 0$ otherwise. However, there is no uniform threshold δ such that the canvas texture can be simply extracted, since the Fourier series coefficients $|\widehat{S}(n)|$ decay when $|n|$ increases. If δ is small, the canvas texture extracted by a uniform thresholding will be contaminated by other fine features of the canvas painting. If δ is large, many Fourier series terms of the canvas would be missed.

This dilemma motivates the design of the multiscale block partition of the frequency domain. Applying the algorithms in Theorem 3.8 in the diffeomorphism based spectral analysis [26], we can estimate the fundamental frequency $N\partial_{x_1}\phi(x)$ in the horizontal direction from the peak positions $\{\xi_{1i}\}$. Similarly, the fundamental frequency $N\partial_{x_2}\phi(x)$ in the vertical direction is estimated. If we denote the estimation of the fundamental frequencies as ω_{hor} and ω_{vert} , respectively, then the frequency domain can be partitioned into multiscale blocks $\{\mathcal{B}_{nm}\}$ with

$$\begin{aligned} \mathcal{B}_{nm} := & \{\xi : (n - 0.5)\omega_{hor} \leq \xi_1 < (n + 0.5)\omega_{hor}, \\ & (m - 0.5)\omega_{vert} \leq \xi_2 < (m + 0.5)\omega_{vert}\} \end{aligned}$$

for integers n and m .

More reasonable than uniform thresholding is then

to threshold $\widehat{\mathcal{I}}^{txt}$ adaptively in each frequency sub-domain $\mathcal{B}_{nm} \cap \mathcal{S}_r$ when $\mathcal{B}_{nm} \cap \mathcal{S}_r \neq \emptyset$. For each pair (n, m) , if $\mathcal{B}_{nm} \cap \mathcal{S}_r \neq \emptyset$, we define an adaptive threshold $\delta_{nm} = \max\{|\widehat{\mathcal{I}}^{txt}(\xi)| : \xi \in \mathcal{B}_{nm} \setminus \mathcal{S}_r\}$. We then define $\widehat{\mathcal{I}}_{est}^c(\xi)$, the estimated spectrum of \mathcal{I}^c , by $\widehat{\mathcal{I}}_{est}^c(\xi) = \widehat{\mathcal{I}}^{txt}(\xi)$ if $|\widehat{\mathcal{I}}^{txt}(\xi)| > \delta_{nm}$ and $\xi \in \mathcal{B}_{nm} \cap \mathcal{S}_r$ and $\widehat{\mathcal{I}}_{est}^c(\xi) = 0$ otherwise. Then \mathcal{I}_{est}^c is able to recover both the high frequency and low frequency components in $\mathcal{I}^c(x) = \sum_{n \in \mathbb{Z}^2} a(x) \widehat{S}(n) e^{2\pi i N n \cdot \phi(x)}$, as illustrated in Fig. 3. Finally, we are able to estimate the canvas part by

$$\mathcal{I}^c \approx \mathcal{I}_{est}^c,$$

The painting part containing fine-scale features such as cracks, brushstrokes, etc. is approximated by

$$\mathcal{I}^p + \mathcal{I}^{out} \approx \mathcal{I} - \mathcal{I}_{est}^c.$$

IV. NUMERICAL RESULTS

The frequency spectrum of (visual-light) photographs and X-ray images of canvas paintings behave very differently, as canvas often dominates in X-ray images while the painting content is usually more prominent in photographs. This difference between both modalities is reflected in the way we identify the frequency components of the canvas. Moreover, because canvas can locally deviate (sometimes significantly) from periodic periodicity, the characteristic frequency components are not localized in peaks, but spread out over frequency ranges, showing up as ridges in the frequency spectrum.

We compare the results of different methods with our proposed algorithm and illustrate the strengths and weaknesses of each, depending on the imaging modality and the type of canvas used. The first method we compare against is Morphological Component Analysis (MCA), using, as its two dictionaries, the discrete cosine transform (DCT) and the dual-tree complex wavelet transform (DT-CWT). For every experiment, the algorithm was run on overlapping blocks of 512×512 pixels with overlapping strips of width 64 pixels. In

principle, the low frequency component could be part of either a DCT or a DT-CWT decomposition. However, since the canvas texture has no low frequency component, we force the low frequency component to be contained entirely in the DT-CWT decomposition, by setting the coarse level DCT coefficients to zero. The second method we compare against is the Wiener filter approach, proposed earlier in [16], which was designed for high-resolution photographs of paintings.

A. High-resolution macrophotography

As explained in Section III, peaks in the two dimensional spectrum are identified by performing peak detection for the (one dimensional) projections of $\widehat{\mathcal{I}}^b = g_{\sigma_1} * \widehat{\mathcal{I}}^{txt} - g_{\sigma_2} * \widehat{\mathcal{I}}^{txt}$ onto the horizontal and vertical axis. For all experiments σ_1 and σ_2 were kept fixed, with $\sigma_1 = 15$, $\sigma_2 = 30$. We observed by experimental evaluation that taking the maximum for each column/row is sufficient to obtain a signal from which we can identify the peaks that correspond to the fundamental frequencies of the canvas in the vertical and horizontal directions respectively. We use the Matlab built-in peak detection function called *findpeaks()*, which measures how much a peak stands out due to its intrinsic height and its location relative to other peaks (we refer the reader to the Matlab documentation for a more detailed explanation). Practically, we limit the number of peaks in each quadrant of the spectrum to 3, in case *findPeaks()* would detect more. Additionally, in case of noisy images where multiple peaks are detected close to each other, we only retain the most prominent peak in a local neighborhood.

a) *Portrait of Suzanne Bambridge (1891)*: This painting of *Paul Gauguin*, depicted in Fig. 1, is painted on rough sackcloth; it is in dire need of restoration and the canvas has become very prominent throughout the years, by dirt accumulation and varnish discoloration. In order to facilitate the analysis of the painting by a professional restorer we were asked to remove canvas

artifacts from the image. Fig. 4 shows a detail from the painting (with dimensions of 512×512 pixels), depicted in Fig. 1, together with the result of the different canvas removal methods mentioned in Section II. The proposed method was run on a selection of the painting with dimensions 2048×2048 pixels and with $r = 4$. While MCA removes the grid structure from the canvas completely, it removes additional features within the image such as brushstrokes and hairline cracks. The Wiener filter method of [16] performs well but some faint canvas structures remain visible; the proposed method, which we refer to as *DeCanv* from now on, removes all canvas structure but does not affect other objects within the painting. Fig. 5 shows two separate details extracted from the results obtained with MCA and *DeCanv*, showing the removed features that one would prefer to see retained.

b) Sandpiper and Pomegranate by Charlotte Caspers (2014): Painting on a coarse, very absorbing jute-type canvas (see Fig. 6(b)). This particular canvas support is much more challenging as its frequency spectrum is more complex, and the peaks, corresponding to different periodic components in different orientations, are more difficult to localize. Fig. 8 shows different canvas removal results by using MCA, Wiener filtering and *DeCanv*, as well as their difference with the original canvas painting. The proposed method was run on a selection of the painting with dimensions 1500×1500 pixels and with $r = 3$. Morphological component analysis removes the entire canvas, but as can be seen from the difference image, it struggles to capture the canvas structure in some areas, such as the top of the image. It also removes some of the fine-scale structures that are part of the original painting. The Wiener filter approach is the least performant as it fails to capture all the frequency components corresponding to the canvas structure. The proposed method *DeCanv* was able to capture the characteristic frequency components of the complex canvas structure, even in areas where the

canvas is difficult to see with the naked eye.

c) Bird by Charlotte Caspers (2014): The painting in Fig. 6(a), originally not on canvas, was painted on a (very smooth) masonite support. The painting was scanned, printed out on canvas and scanned again; the hope was that this would provide an image with visual canvas structure for which we also knew the canvas-free ground truth. The printing and scanning steps, however, distorted the color distribution of the image quite significantly and introduced spatial distortions. For a reasonably fair comparison of the original image with the different canvas removal results, a registration (i.e. spatial alignment) step as well as a color remapping of the results to the original was required. Fig. 8 shows our attempt at comparing different canvas removal methods with the ground-truth data depicted in Fig. 8(a). It has to be noted that the digital processing required to create the canvassed version of this painting introduced noise, which is not present in the original. MCA, also used as a denoising technique, quite successfully removes the introduced noise, together with the canvas texture and some of the thinner brushstrokes. It is difficult in this case to distinguish a difference in performance between the results obtained with Wiener filtering and *DeCanv*. They both successfully remove the faint canvas without affecting other structures in the image. Our method was run on blocks of 1024×1024 pixels with $r = 2$.

B. X-ray imaging

As mentioned in the introduction of this section, canvas structure is much more prominent and sharply delineated in X-ray images of old paintings: typically their lead-containing primer accumulated more in the spaces between the canvas threads, so that variations in X-ray penetration, due to these variations in thickness of the X-ray absorbing primer layer, provide a clear “imprint” of the canvas structure. To the best of the authors’ knowledge, the removal of canvas structures from X-ray images of paintings has not been attempted

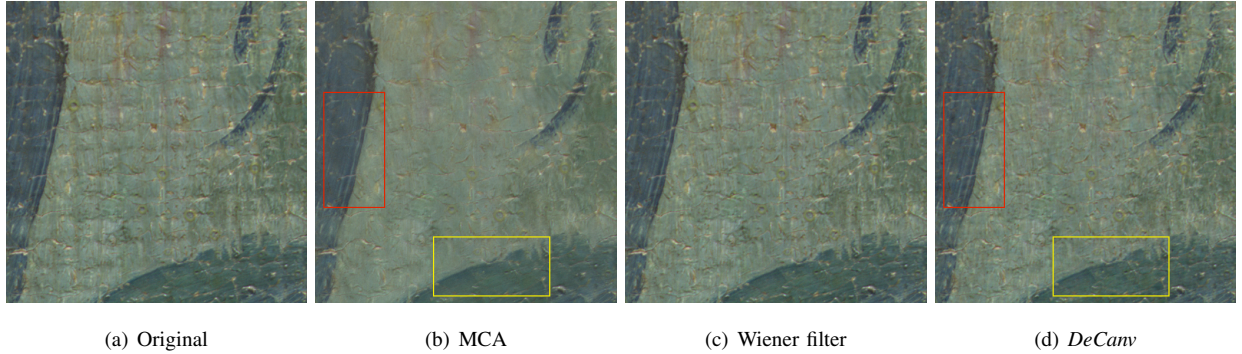


Fig. 4. *Portrait of Suzanne Bambridge* (1891): Canvas removal results on image (a) with MCA (b), smoothing Wiener filter (c) and the proposed method, called *DeCanv* (d) respectively.

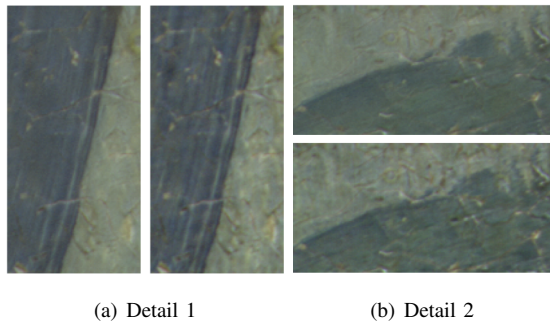


Fig. 5. *Portrait of Suzanne Bambridge* (1891): Comparison on two details between MCA ((a) left and (b) top) and *DeCanv* ((a) right and (b) bottom).

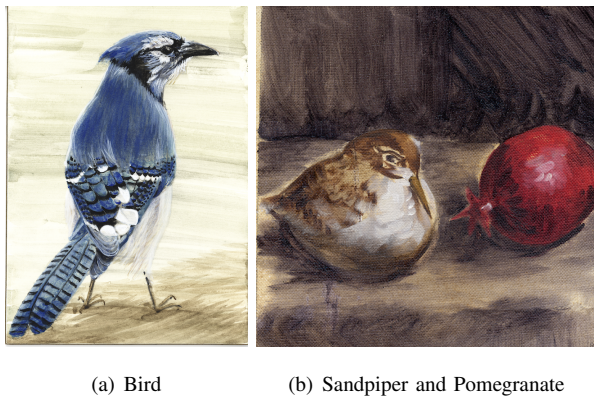


Fig. 6. Still-life paintings by Charlotte Caspers, originally made for digital brushstroke analysis studies.

before. Nevertheless, it may facilitate the reading of the X-ray image by experts interested in decoding clues to the realization or the state of conservation of the painting, and as such this technique is of interest to art conservators. Similarly to the visual-light photographs discussed earlier, one can detect frequency peaks that correspond to the fundamental frequencies of the canvas weave by examining the projections on the horizontal and vertical axis of the Fourier spectrum of the X-ray images. These peaks tend to be less well-localized in the frequency domain, but spread out more, forming ridges; reliable peak detection can still be achieved by first summing the spectral contributions in each row and column and identifying the local maxima of these marginal 1-D distributions (instead of locating local maxima for the 2-D distributions, as was done earlier).

a) The Virgin and Child with St. John and His Parents (1617): Fig. 9 shows a detail (with 1800×1300 pixels) of this oil painting on canvas by Jacob Jordaens, currently residing in the collection of the North Carolina Museum of Art, before (a) and after (b) the canvas has been removed with the proposed method. To obtain this final result, the vertical stretcher bar was removed first with the algorithm presented in [12] and subsequently the canvas texture was removed with *DeCanv* on overlapping blocks of 512×512 with overlapping strips of 128 pixels wide, and with $r = 4$. Fig. 10

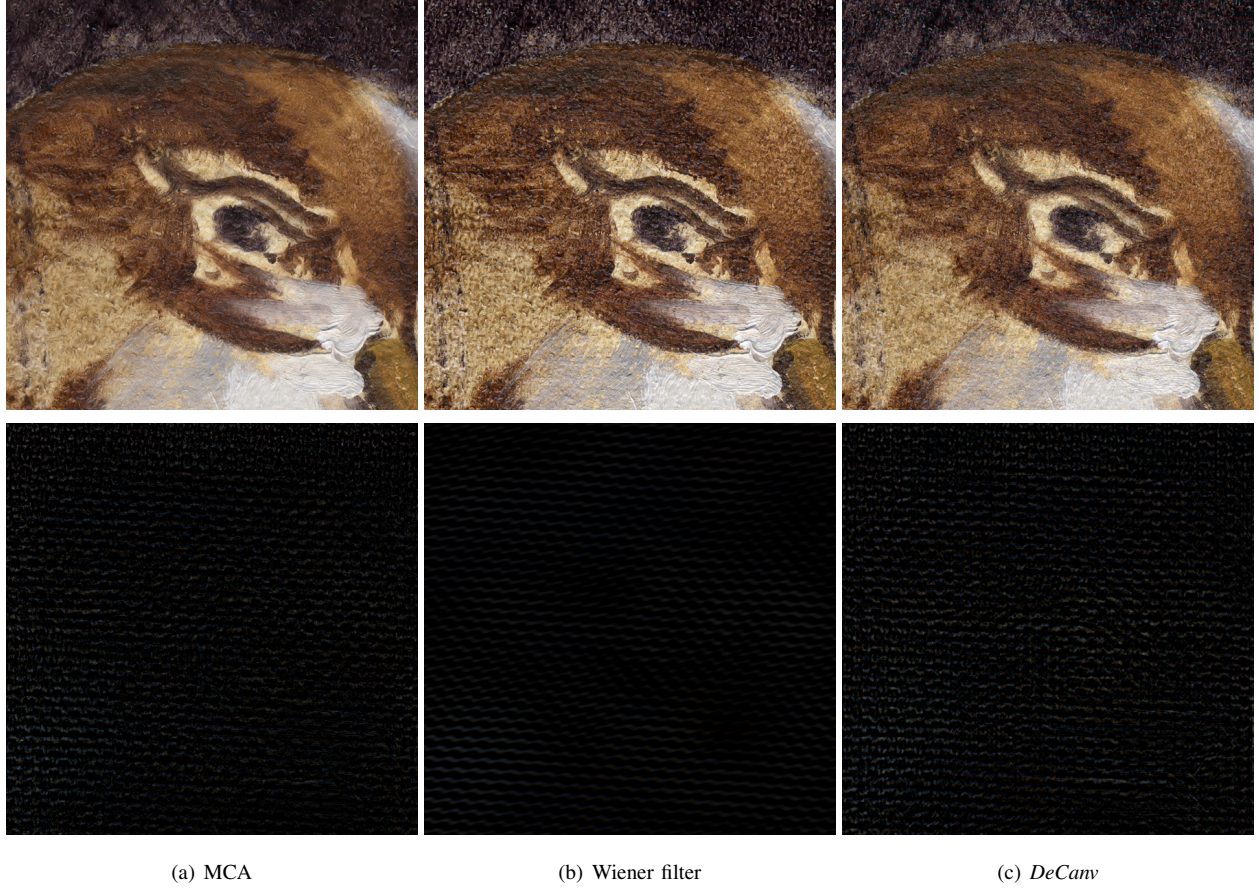


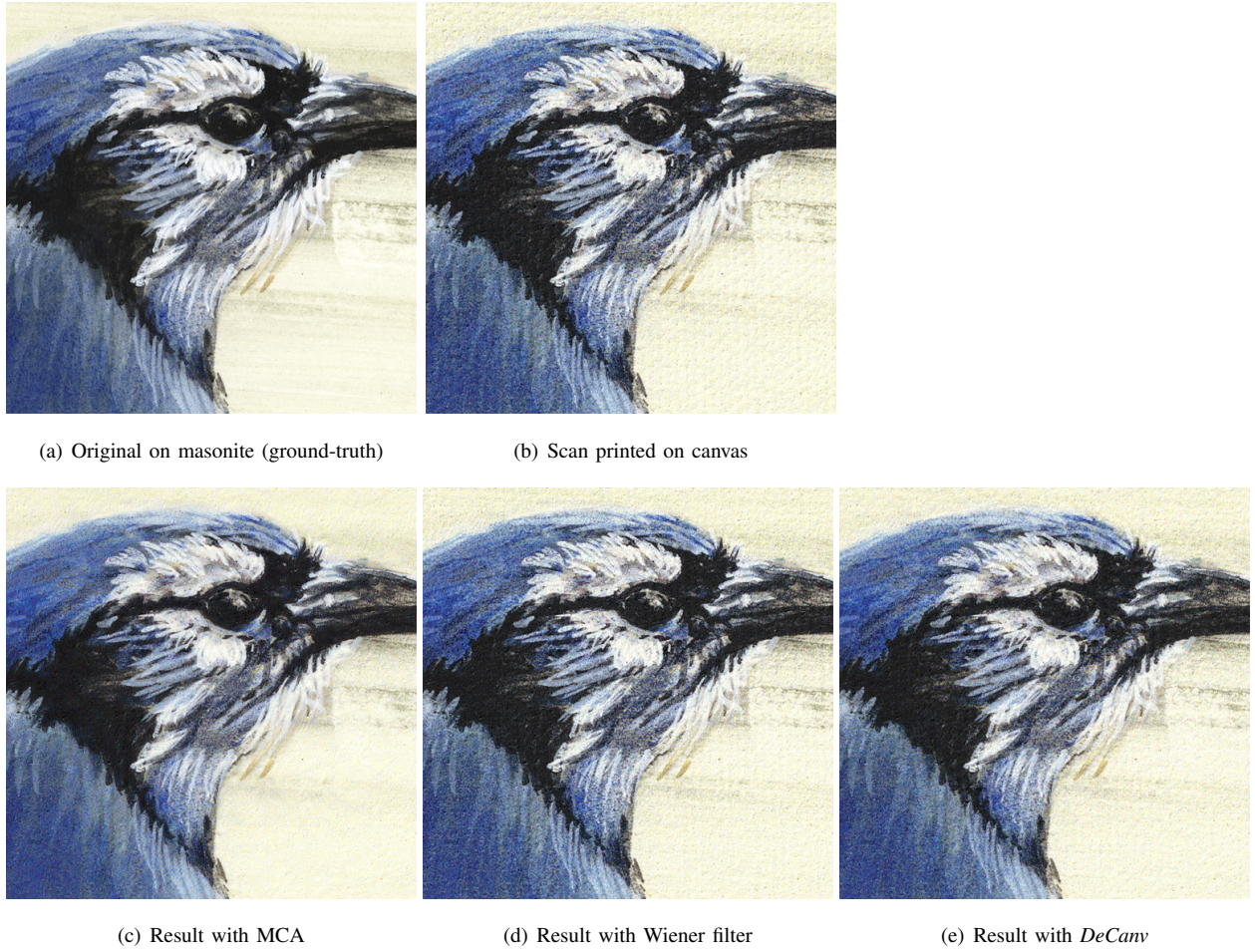
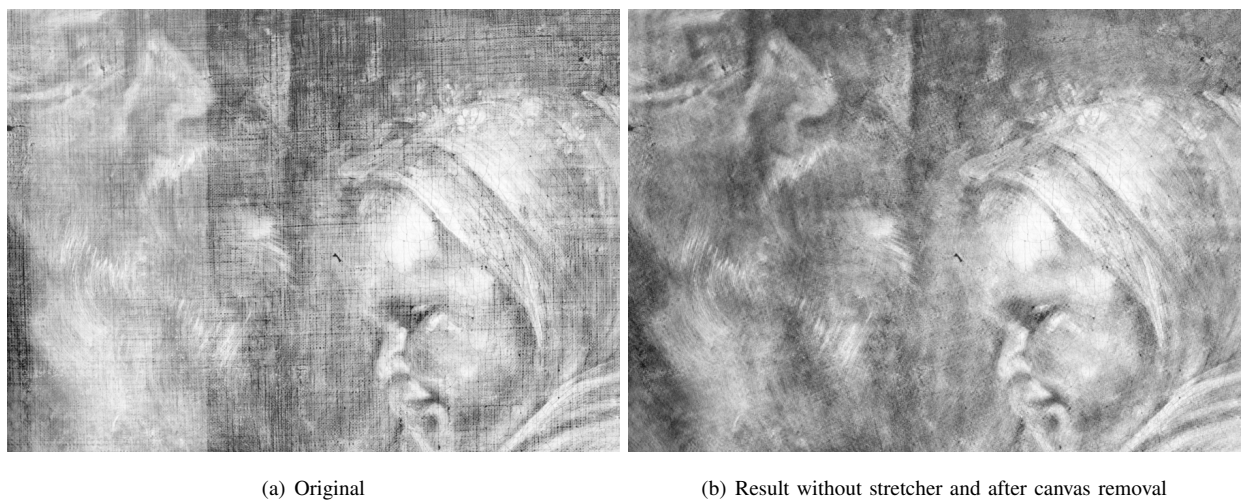
Fig. 7. Canvas removal results and their difference with original canvas painting entitled *Sandpiper and Pomegranate* by *Charlotte Caspers*.

shows results with competing methods on a zoom-in. The Wiener filter fails to capture the prominent and complex structure of the canvas and removes only the lower frequency components from the canvas spectrum, which is clearly insufficient for X-ray images. It also deals poorly with the local deviations from periodicity of the canvas. MCA does a much better job at removing the canvas texture, but it has a tendency to smooth out the image and remove some of the fine-scale details that are captured by the DCT dictionary. Overall, *DeCanv* performs best, clearly removing the canvas pattern, while leaving the fine-scale details intact. This observation is corroborated by the result in Fig. 11, showing a different zoom-in, from an area where the stretcher is located.

b) Portrait of an Old Man with Beard (1885):

This painting by *van Gogh*, currently residing in the collection of the Van Gogh Museum in Amsterdam, has a much coarser canvas that is distorted in some places, especially at the edges, where it is attached to the stretcher. Fig. 12 depicts a selection from the painting alongside its canvas-free version and the retrieved canvas component, obtained with $r = 3$. From the difference image it is clear that only the canvas is extracted. The proposed method is thus also capable of capturing these strong deviations in the periodicity of the canvas.

c) Lady Mary Villiers, Later Duchess of Richmond and Lennox (1637): This painting by the Dutch artist *Anthony van Dyck* is currently in the collection of the

Fig. 8. Canvas removal results on bird painting by *Charlotte Caspers*.Fig. 9. *The Virgin and Child with St. John and His Parents*: (left) original - (right) after removal of the stretcher and canvas.

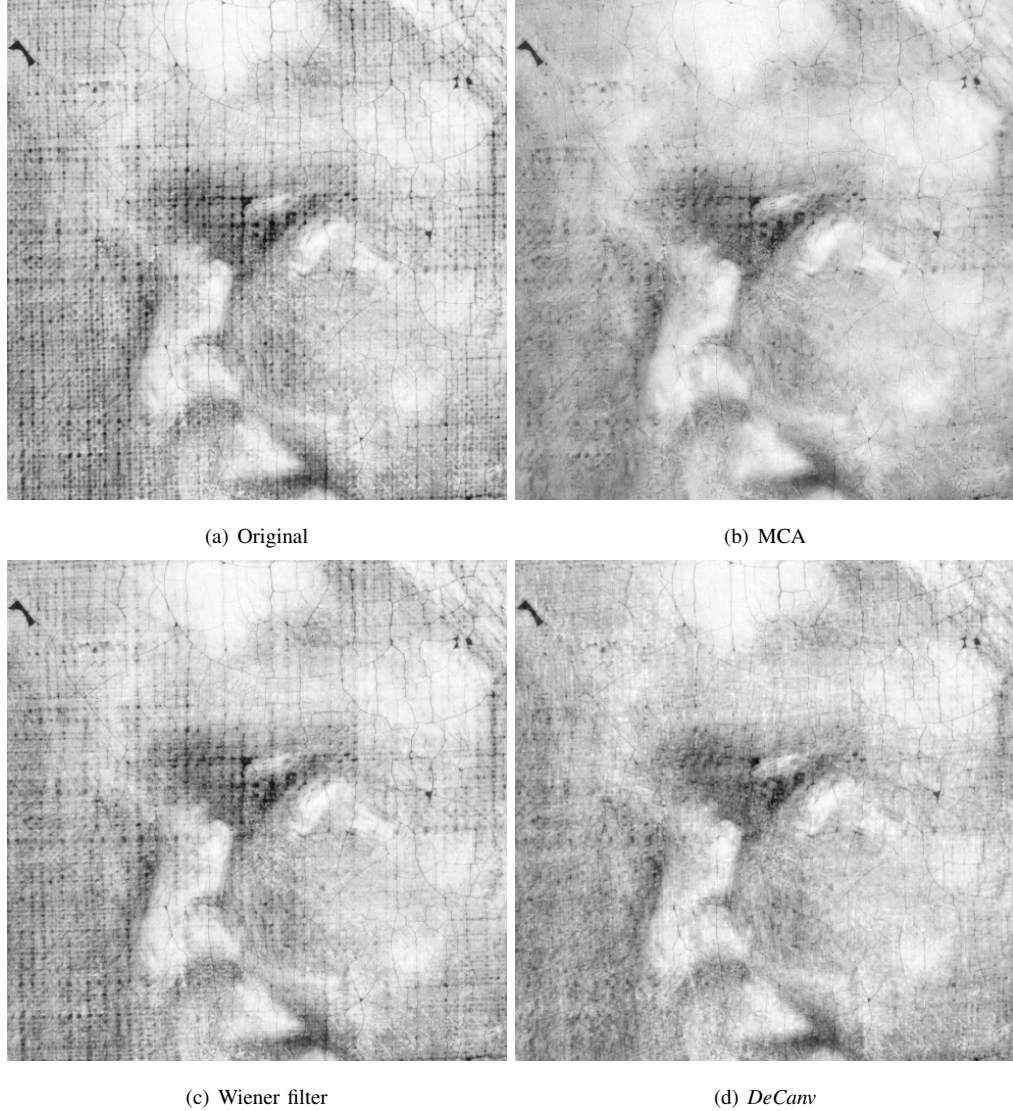


Fig. 10. Canvas removal results on detail of *The Virgin and Child with St. John and His Parents*

NCMA. Fig. 13 contains the different canvas removal results on a detail of the painting. The original X-ray image contains a very prominent canvas structure while the painting content itself appears faded. It is clear from Fig. 13(c) that the Wiener filter is not the adequate method for the separation of the canvas from the painting. MCA performs decently but fails to extract canvas in places where it is very dominant. *DeCanv* was performed on the original crop of size 1360×1380 with $r = 4$.

C. Note on post-processing

Depending on the acquisition settings and the processing done at the museum (which might differ strongly from one image to another), images can be very contrasted and/or saturated, especially in X-ray images. Strongly saturated areas do not respond well to any form of digital processing and are prone to the introduction of undesirable artifacts. Such areas are detected in the original image \mathcal{I} by thresholding a blurred version of the original, with a very large threshold close to the

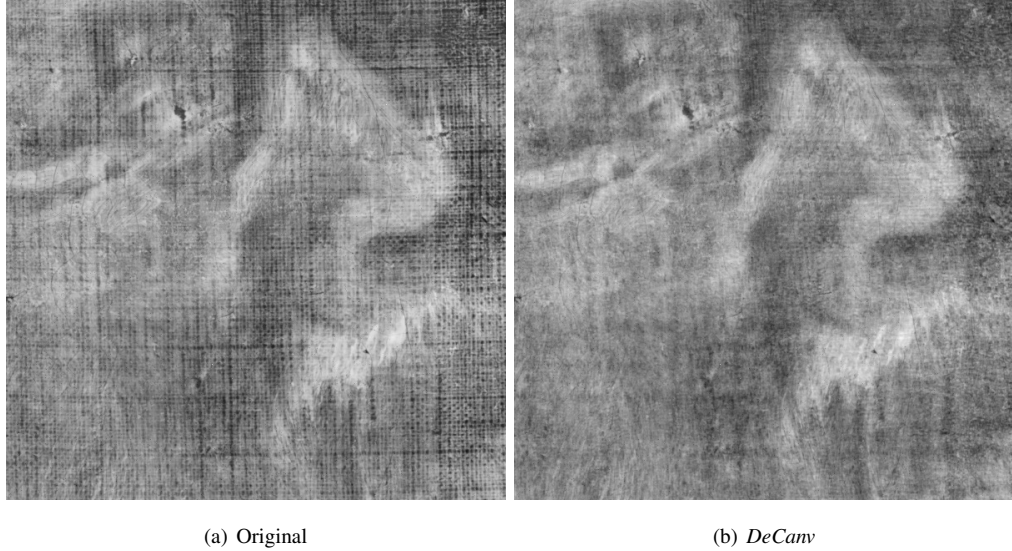


Fig. 11. Canvas removal results on detail of *The Virgin and Child with St. John and His Parents*

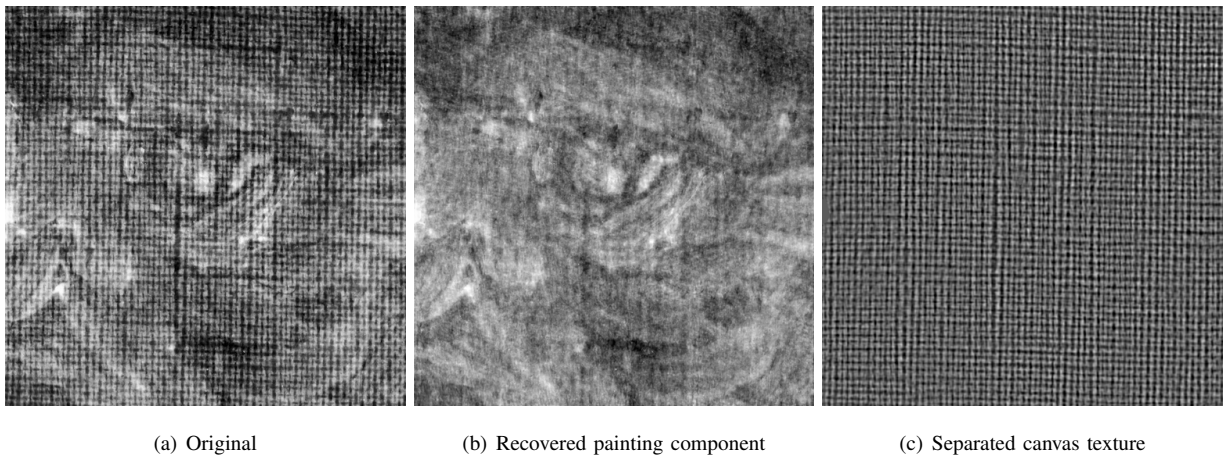


Fig. 12. *Portrait of an Old Man with Beard*: canvas removal results and the difference with original canvas painting.

maximum intensity value. Large saturated areas are replaced in the result with their original. An example of such processing is depicted in Fig. 10, where the forehead of the baby is very bright and does not contain canvas.

V. CONCLUSIONS AND FUTURE WORK

We introduce *DeCanv*, a source separation method for the removal of periodic structures, and applied it in the context of the novel application of canvas removal from digital image acquisitions of paintings on canvas. The

nature of the canvas is very specific and behaves very differently depending on the acquisition modality. Especially for X-ray images, classic methods for (quasi-) periodic noise removal fail because the fundamental frequency components of the canvas spectrum are not well localized into peaks but rather spread out over ridges. Wholesale removal of high-frequency content, while removing the canvas structures, blurs sharp edges in the image. Hence, we propose a two-stage method that first decomposes the image into cartoon and texture

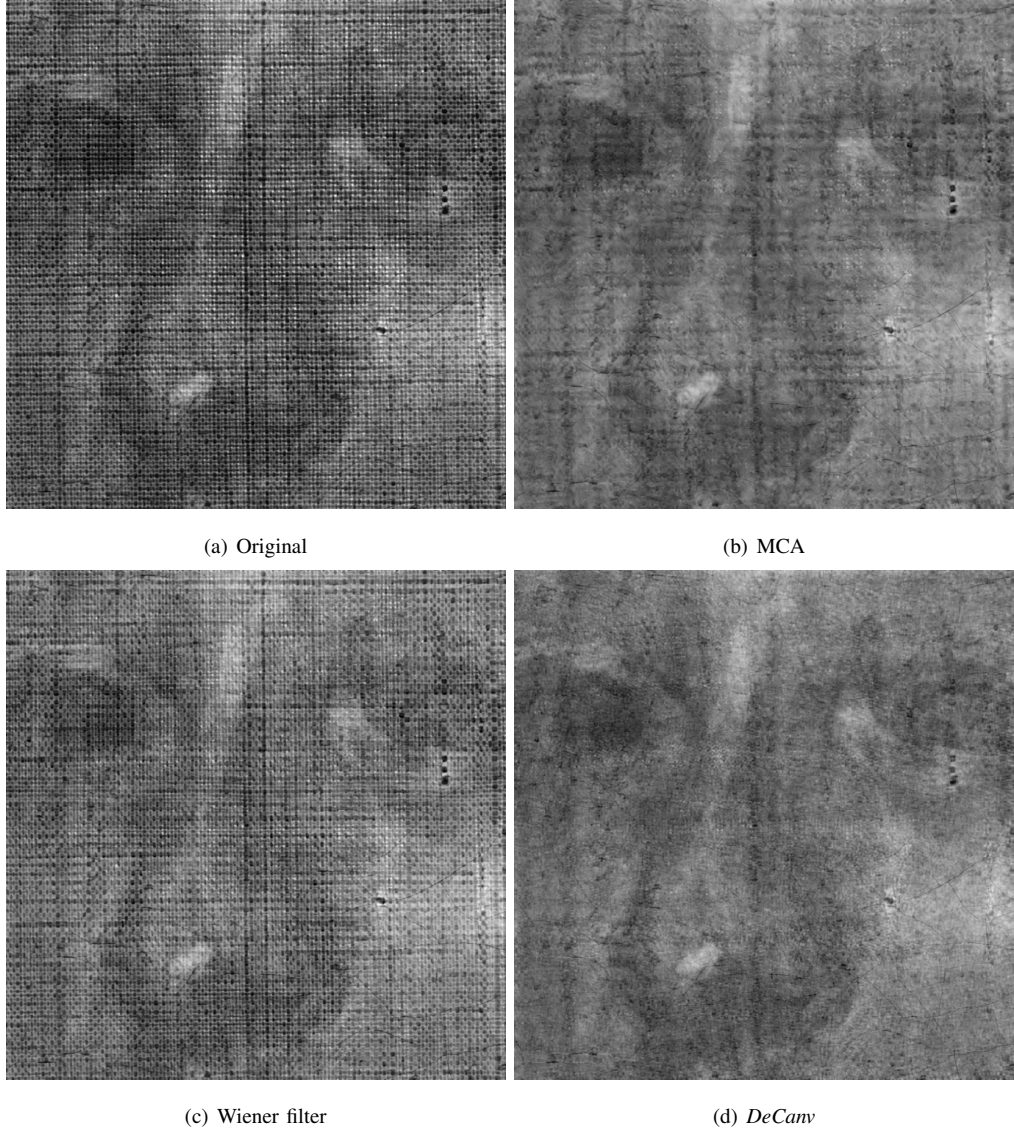


Fig. 13. Canvas removal results on detail of *Lady Mary Villiers, Later Duchess of Richmond and Lennox*.

parts, minimally affecting the stronger edges that belong to the pictorial content of the painting. The second processing step targets the texture component; it uses adaptive multiscale thresholding in the frequency domain to specifically target and suppress the frequency components of the canvas. Results were compared to those obtained with other well-known competing methods and assessed visually by an art expert (co-author N. Ocon of this manuscript). Our new method performs better than previous methods in various complicated

examples.

We note that the canvas removal technique was used in [33], which re-examined earlier results obtained by one of us in collaboration with others [1], in a study of distinguishing original paintings from copies; [33] specifically studied whether the positive results of [1] could be explained, in part, by a recognition of the canvas rather than the painting technique.

The following are some possible research directions to improve on the current approach. First, the peak

position estimation by one-dimensional projection in the second stage is not very robust under very significant image rotations and other heavy deformations. In these cases, it might be better to apply the highly redundant two-dimensional synchrosqueezed transform [34] to estimate the rotation and the deformation of the canvas. Once this information is available, one can rotate and deform the canvas back to standard canvas texture with straight horizontal and vertical threads. The canvas removal algorithm introduced in this paper can then be applied to remove the canvas texture afterwards. Second, the estimated canvas texture \mathcal{I}_{est}^c may violate the model $a(x)S(2\pi N\phi(x))$ for some smooth amplitude and phase functions. A possible solution is to extend the one-dimensional diffeomorphism spectral analysis method in [26] to a two-dimensional method to estimate $N\phi(x)$, $S(x)$ and $a(x)$ from the removed canvas texture. A post-processing technique based on variational optimization, presented in [35], may further refine these estimations such that they agree better with the canvas model, i.e., $\mathcal{I}_{est}^c \approx a(x)S(2\pi N\phi(x))$ with a smooth amplitude $a(x)$, a smooth deformation $\phi(x)$ and $\text{curl}\nabla\phi = 0$.

ACKNOWLEDGMENT

The work of J.L. was supported in part by the National Science Foundation under award DMS-1454939 and the Alfred P. Sloan foundation. H.Y. thanks the support of National Science Foundation under award ACI-1450372 and AMS-Simons Travel Award. The authors would like to thank the North Carolina Museum of Arts, as well as the *Van Gogh* museum in Amsterdam for generously providing the visual material for this study.

REFERENCES

- [1] C. R. Johnson, E. Hendriks, I. J. Berezhnoy, E. Brevdo, S. M. Hughes, I. Daubechies, J. Li, E. Postma, and J. Z. Wang, “Image processing for artist identification,” *Signal Processing Magazine, IEEE*, vol. 25, no. 4, pp. 37–48, 2008.
- [2] P. Abry, S. Roux, H. Wendt, P. Messier, A. Klein, N. Tremblay, P. Borgnat, S. Jaffard, B. Vedel, J. Coddington, and L. Daffner, “Multiscale anisotropic texture analysis and classification of photographic prints: Art scholarship meets image processing algorithms,” *Signal Processing Magazine, IEEE*, vol. 32, no. 4, pp. 18–27, July 2015.
- [3] N. van Noord, E. Hendriks, and E. Postma, “Toward discovery of the artist’s style: Learning to recognize artists by their artworks,” *Signal Processing Magazine, IEEE*, vol. 32, no. 4, pp. 46–54, July 2015.
- [4] D. Johnson, C. Johnson Jr., A. Klein, W. Sethares, H. Lee, and E. Hendriks, “A thread counting algorithm for art forensics,” in *Digital Signal Processing Workshop and 5th IEEE Signal Processing Education Workshop, 2009. DSP/SPE 2009. IEEE 13th*, Jan 2009, pp. 679–684.
- [5] D. H. Johnson, J. C. R. Johnson, and R. G. Erdmann, “Weave analysis of paintings on canvas from radiographs,” *Signal Processing*, vol. 93, no. 3, pp. 527 – 540, 2013, image Processing for Digital Art Work.
- [6] H. Yang, J. Lu, W. Brown, I. Daubechies, and L. Ying, “Quantitative canvas weave analysis using 2-D synchrosqueezed transforms: Application of time-frequency analysis to art investigation,” *Signal Processing Magazine, IEEE*, vol. 32, no. 4, pp. 55–63, July 2015.
- [7] L. van der Maaten and R. Erdmann, “Automatic thread-level canvas analysis: A machine-learning approach to analyzing the canvas of paintings,” *Signal Processing Magazine, IEEE*, vol. 32, no. 4, pp. 38–45, July 2015.
- [8] B. Cornelis, T. Ružić, E. Gezels, A. Dooms, A. Pižurica, L. Platiša, J. Cornelis, M. Martens, M. De Mey, and I. Daubechies, “Crack detection and inpainting for virtual restoration of paintings: The case of the Ghent Altarpiece,” *Signal Processing*, 2012.
- [9] B. Cornelis, Y. Yang, J. T. Vogelstein, A. Dooms, I. Daubechies, and D. Dunson, “Bayesian crack detection in ultra high resolution multimodal images of paintings,” *arXiv preprint arXiv:1304.5894*, 2013.
- [10] A. Pizurica, L. Platiša, T. Ruzic, B. Cornelis, A. Dooms, M. Martens, H. Dubois, B. Devolder, M. D. Mey, and I. Daubechies, “Digital image processing of the Ghent Altarpiece: Supporting the painting’s study and conservation treatment,” *IEEE Signal Processing Magazine*, vol. 32, p. 11, Jun 2015.
- [11] R. Yin, D. Dunson, B. Cornelis, B. Brown, N. Ocon, and I. Daubechies, “Digital cradle removal in x-ray images of art

- paintings,” in *Image Processing (ICIP), 2014 IEEE International Conference on*, Oct 2014, pp. 4299–4303.
- [12] R. Yin, B. Cornelis, G. Fodor, D. Dunson, and I. Daubechies, “Digital cradle removal in X-ray images of Art Paintings,” *SIAM Journal on Imaging Sciences (SIIMS) - submitted*, 2015.
- [13] C. Christensen, “The Painting Materials and Technique of Paul Gauguin,” *Conservation Research, Monograph Series II, Studies in the History of Art*, vol. 41, pp. 63–103, 1993.
- [14] B. Cornelis, A. Dooms, F. Leen, A. Munteanu, and P. Schelkens, “Multispectral imaging for digital painting analysis: a Gauguin case study,” in *Proc. of SPIE, Applications of Digital Image Processing XXXIII*, vol. 7798, San Diego, USA, 2010.
- [15] B. Cornelis, A. Dooms, A. Munteanu, J. Cornelis, and P. Schelkens, “Experimental study of canvas characterization for paintings,” in *Proc. of IS&T/SPIE Electronic Imaging 2010*, vol. 7531, San Jose, CA, USA, 2010.
- [16] B. Cornelis, A. Dooms, J. Cornelis, and P. Schelkens, “Digital canvas removal in paintings,” *Signal Processing*, vol. 92, no. 4, pp. 1166–1171, 2012.
- [17] I. Aizenberg and C. Butakoff, “Frequency domain median-like filter for periodic and quasi-periodic noise removal,” *Proceedings of SPIE*, pp. 181–191, 2002. [Online]. Available: <http://link.aip.org/link/?PSI/4667/181/1&Agg=doi>
- [18] G. A. Hudhud and M. Turner, “Digital removal of power frequency artifacts using a Fourier space median filter,” *IEEE Signal Processing Letters*, vol. 12, no. 48, pp. 573–576, 2005.
- [19] I. Aizenberg and C. Butakoff, “A windowed gaussian notch filter for quasi-periodic noise removal,” *Image Vision Comput.*, vol. 26, pp. 1347–1353, October 2008. [Online]. Available: <http://portal.acm.org/citation.cfm?id=1405206.1405432>
- [20] J. I. Starck, M. Elad, and D. Donoho, “Image decomposition via the combination of sparse representations and a variational approach,” *IEEE Transactions on Image Processing*, vol. 14, pp. 1570–1582, 2004.
- [21] J. Bobin, J. L. Starck, J. M. Fadili, Y. Moudden, and D. L. Donoho, “Morphological Component Analysis: An Adaptive Thresholding Strategy,” *IEEE Transactions on Image Processing*, vol. 16, no. 11, pp. 2675–2681, Nov. 2007.
- [22] N. G. Kingsbury, “The dual-tree complex wavelet transform: a new technique for shift invariance and directional filters,” in *Proc. 8th IEEE DSP Workshop*, vol. 8. Citeseer, 1998, p. 86.
- [23] H. Yang, J. Lu, and L. Ying, “Crystal image analysis using 2D synchrosqueezed transforms,” *Multiscale Modeling & Simulation*, vol. 13, no. 4, pp. 1542–1572, 2015. [Online]. Available: <http://dx.doi.org/10.1137/140955872>
- [24] H. Yang and L. Ying, “Synchrosqueezed wave packet transform for 2d mode decomposition,” *SIAM Journal on Imaging Sciences*, vol. 6, no. 4, pp. 1979–2009, 2013. [Online]. Available: <http://dx.doi.org/10.1137/120891113>
- [25] —, “Synchrosqueezed curvelet transform for two-dimensional mode decomposition,” *SIAM Journal on Mathematical Analysis*, vol. 46, no. 3, pp. 2052–2083, 2014.
- [26] H. Yang, “Synchrosqueezed wave packet transforms and diffeomorphism based spectral analysis for 1d general mode decompositions,” *Applied and Computational Harmonic Analysis*, vol. 39, no. 1, pp. 33 – 66, 2015.
- [27] C. K. Chui, Y.-T. Lin, and H.-T. Wu, “Real-time dynamics acquisition from irregular samples – with application to anesthesia evaluation,” *Analysis and Applications*, Accepted.
- [28] Y. Meyer, *Oscillating patterns in image processing and nonlinear evolution equations: the fifteenth Dean Jacqueline B. Lewis memorial lectures*. American Mathematical Soc., 2001, vol. 22.
- [29] D. Mumford and J. Shah, “Optimal approximations by piecewise smooth functions and associated variational problems,” *Communications on pure and applied mathematics*, vol. 42, no. 5, pp. 577–685, 1989.
- [30] L. I. Rudin, S. Osher, and E. Fatemi, “Nonlinear total variation based noise removal algorithms,” *Physica D: Nonlinear Phenomena*, vol. 60, no. 1, pp. 259–268, 1992.
- [31] T. F. Chan and S. Esedoglu, “Aspects of total variation regularized 1 1 function approximation,” *SIAM Journal on Applied Mathematics*, vol. 65, no. 5, pp. 1817–1837, 2005.
- [32] A. Buades, T. M. Le, J.-M. Morel, L. Vese *et al.*, “Fast cartoon+texture image filters,” *Image Processing, IEEE Transactions on*, vol. 19, no. 8, pp. 1978–1986, 2010.
- [33] G. Wang, H. Wendt, P. Abry, I. Daubechies, and S. Jaffard, “A review of forgery detection in paintings, with new discoveries,” *in preparation*, 2016.
- [34] H. Yang, “Robustness analysis of synchrosqueezed transforms,” *arXiv:1410.5939 [math.ST]*, 2014, preprint. [Online]. Available: <http://arxiv.org/abs/1410.5939>
- [35] J. Lu, B. Wirth, and H. Yang, “Combining 2D synchrosqueezed wave packet transform with optimization for crystal image analysis,” *Journal of the Mechanics and Physics of Solids*, pp. –, 2016. [Online]. Available: <http://www.sciencedirect.com/science/article/pii/S0022509616300023>

Bruno Cornelis (bcorneli@math.duke.edu) received the M.S. degree of Industrial Engineer in Electronics from Erasmushogeschool Brussel, Belgium, in 2005 and the M.S. degree in Electrical Engineering from Vrije Universiteit Brussel (VUB), Belgium, in 2007. He obtained a Ph.D. degree in Applied Sciences and Engineering from VUB in 2014. During his Ph.D. he investigated the use of various image processing tools in support of art scholarship. His research interests include statistical data analysis and sparse representations in image processing. Currently he is a visiting assistant professor in the Mathematics Department at Duke University.

Noelle Ocon received her undergraduate degree in Art History in 1990 from the University of North Carolina-Chapel Hill, concentrating on Northern European art of the 16th and 17th Centuries. Following an apprenticeship in Washington, D.C. she entered the Art Conservation Program at State University College at Buffalo, NY in 1993. After interning at the Philadelphia Museum of Art and the Indianapolis Museum of Art, she graduated with a Masters of Art with a certificate of advanced studies in conservation in 1996. Ms. Ocon accepted a position in the conservation department at the NCMA in 1997, where her main focus is research and treatment of the permanent collection, with contributions to the Systematic Catalogue of the Dutch and Flemish Collection and Egyptian Collection, and the upcoming Systematic Catalogues for the Classical and Northern Renaissance collections. Another focus is that of technology in the examination and documentation of paintings, including infrared reflectography and x-radiography.

Haizhao Yang (haizhao@math.duke.edu) is currently a visiting assistant professor in the Mathematics Department at Duke University. Before joining Duke University, he received the B.S. degree from Shanghai Jiao Tong University in 2010, the M.S. degree from the University of Texas at Austin in 2012, and the Ph.D. degree from Stanford University all in mathematics.

Jianfeng Lu (jianfeng@math.duke.edu) is an Assistant Professor of Mathematics, Chemistry, and Physics at Duke University. He received the B.S. degree in mathematics from Peking University in 2005 and the Ph.D. degree in applied mathematics from Princeton University in 2009. Before joining Duke University in 2012, he was a Courant Instructor at New York University.

Alex Goodfriend (alexgoodfriend@gmail.com) received an M.S. in Applied Mathematics from the University of Washington, Seattle, Washington USA in 2014. His current research interests include ecological modelling and data analysis as tools to inform environmental policy.

Ingrid Daubechies (ingrid@math.duke.edu) is a James B. Duke Professor of Mathematics at Duke University. She received her B.S. and Ph.D. degrees in Physics for the Vrije Universiteit Brussel (Belgium), where she also started her research career. In the USA, she has previously been at AT&T Bell Labs (1987-94), at Rutgers University (1991-93) and at Princeton (1994-2010). She is a Fellow of the IEEE. She received the Benjamin Franklin Medal for Electrical Engineering and the James Kilby Medal of the IEEE Signal Processing Society, both in 2011.